Infrared Vibrational Intensities, Polar Tensors, and Core Electron Energies of the Group IV Hydrides and the Fluorosilanes

Anselmo E. de Oliveira, Paulo H. Guadagnini, Rogério Custódio,[†] and Roy E. Bruns*[,‡]

Instituto de Química, Universidade Estadual de Campinas, CP 6154, 13081-970 Campinas, SP, Brazil

Received: October 23, 1997; In Final Form: April 3, 1998

Principal component analysis is used to compare polar tensors of CH_4, SiH_4, GeH_4, and SnH_4 and their completely deuterated analogues determined from infrared fundamental gas-phase intensities measured in different laboratories. This analysis also includes theoretical polar tensor values obtained from effective core potential universal basis set calculations as well as from MP2/6-311++G(3d,3p) functions for CH_4, SiH_4, and SiF_4. Theoretical values are also used to resolve sign ambiguities in the dipole moment derivatives of SiF_4. Preferred polar tensor values are proposed for all these molecules. Mean dipole moment derivatives for SiH_4 and SiF_4 are related to the 2p core ionization energies using the simple potential model proposed by Siegbahn and collaborators. These results are confirmed by MP2/6-311++G(3d,3p) calculations for these molecules and for SiH_3F, SiH_2F_2, and $SiHF_3$. This study is extended to the fluorogermanes using experimental 3p and 3d core electron ionization energies and mean dipole moment derivatives calculated from MP2/A-VDZ/6-311++G(3d,3p) wave functions. The simple potential model interpretation of mean dipole moment derivatives as atomic charges implies that the silicon charge, ±0.904e, is slightly higher than the germanium charge of ±0.862*e*.

Introduction

Recently the mean dipole moment derivatives of the carbon atoms of a large and diverse group of molecules have been related to their 1s carbon electron energies[1] using the simple potential model originally proposed by Siegbahn and co-workers[2] to interpret X-ray photoelectron spectra. This result suggests that these mean dipole moment derivatives determined using measured infrared fundamental gas-phase intensities and normal coordinate transformations obtained from empirical force fields can be interpreted as atomic charges. As a consequence, it is of interest to determine whether the *n*p core electron energies of the other group IV atoms are also related in the same way to polar tensor data. Although a large quantity of X-ray photoelectron spectroscopic data exists for free molecules, complete gas-phase infrared fundamental intensity data are available for very few molecules containing group IV atoms heavier than carbon. This limits attempts to relate their vibrational intensity parameters to X-ray photoelectron results.

Infrared intensities have been measured some time ago for the group IV hydrides, CH_4,[3−6] SiH_4,[7,8] GeH_4,[9,10] and SnH_4,[11,12] and recently the silane, germane, and stannane intensities have been determined again.[13] Polar tensors for these molecules have also been reported in the latter reference. Here, principal component analysis[14] is used to compare the polar tensor values obtained from the different sets of experimental intensities. Furthermore these values are compared with theoretical results obtained from ab initio calculations with the aim of resolving sign ambiguities in the dipole moment derivatives with respect to normal coordinates. Preferred polar tensor values obtained from this analysis are then proposed for these molecules. These values are of special interest since diverse chemical evidence indicates that the Si, Ge, and Sn atoms are much more positive than the carbon one.[15] As such one might expect that their mean dipole moment derivatives are considerably higher than the carbon mean derivatives in analogous compounds, for example the fluoromethanes and fluorosilanes.

The tetrafluorosilane fundamental IR intensities have also been measured in the gas phase[16] and with the experimental silane intensities provide an opportunity to test whether the 2p silicon electron core energies and the silicon mean dipole moment derivatives of SiH_4 and SiF_4 can be related by the potential model. However a rigorous test of the use of spectral parameters in this model should use data for the mono-, di-, and trifluoro-substituted silanes for which the infrared intensities and 2p silicon core energies have not been measured. For this reason ab initio calculations are also used here to estimate the silicon 2p core electron binding energies. The experimental results for SiH_4 and SiF_4 and ab initio calculated energies and mean dipole moment derivatives of these molecules and other fluorosilanes are then applied to the potential model equation. A comparison of this equation with the potential equation already determined for the fluoromethanes is then made.

In summary, multivariate statistical analysis and ab initio molecular orbital results are employed to determine unique sets of polar tensor elements from the MH_4 (M = C, Si, Ge, and Sn) and SiF_4 infrared intensities and normal coordinates. ΔSCF values of the 2p electron binding energies and theoretical polar tensor values of the Si atom in SiH_4 and SiF_4 are compared with experimental results. These results and ab initio results for fluorine-substituted silanes (SiH_xF_y; $x, y = 0, 1, 2, 3, 4$ and $x + y = 4$) are interpreted in the light of experimental results already reported for the fluoromethanes and other carbon-containing molecules.[17]

Calculations

The values of infrared-active fundamental frequencies and intensities along with the symmetrized force fields were taken

[†] roger@iqm.unicamp.br.
[‡] bruns@iqm.unicamp.br.

S1089-5639(97)03437-3 CCC: $15.00
Published on Web 05/22/1998

TABLE 1: Observed Intensities and Fundamental Frequencies for the Group IV Hydrides and SiF_4

	CH_4	CD_4	SiH_4	SiD_4	GeH_4	GeD_4	SnH_4	SnD_4	SiF_4
					Frequencies (cm^{-1})				
ν_3	3019[a]	2259[a]	2190.6[f]	1597[f]	2113.6[i]	1522.2[i]	1901.1[k]	1367.5[k]	1028[m]
			2189.19[g]		2111.58[g]		1905.68[g]		
			2189.2[h]	1598.3[h]	2111.8[j]		1905.89[l]		
ν_4	1306[a]	996[a]	914.2[f]	681[f]	819.3[i]	596[i]	677[k]	487[k]	388.58[m]
			913.47[g]		821.11[g]		680.78[g]		
			914.1[h]	675[h]	819.3[j]		679[l]		
					Intensities ($km.mol^{-1}$)				
A_3	69.7 ± 2.1[b]	33.1 ± 1.0[b]	320.5 ± 0.9[f]	127.1 ± 3.4[f]	313 ± 8[i]	171.4 ± 0.9[i]	922.2 ± 12.4[k]	460.0 ± 5.1[k]	591 ± 59[n]
	68.0 ± 2.0[c]	30.1 ± 1.0[c]	282 ± 3[g]		332 ± 7[g]		444 ± 3[g]		
	65.5 ± 0.9[d]	28.8 ± 1.4[d]	304[h]	177[h]	302[j]		456[l]		
	66.8 ± 0.2[e]	29.8 ± 0.9[e]							
A_4	33.4 ± 1.0[b]	19.0 ± 0.6[b]	296.4 ± 21.7[f]	136.5 ± 8.3[f]	281.7 ± 4.0[i]	137.2 ± 1.1[i]	778.3 ± 13.1[k]	419.1 ± 26.5[k]	114 ± 11[n]
	36.0 ± 1.0[c]	19.8 ± 0.4[c]	381 ± 4[g]		283 ± 6[g]		406 ± 4[g]		
	31.8 ± 0.6[d]	18.4 ± 0.5[d]	399[h]	209[h]	245[j]		342[l]		
	32.7 ± 0.5[e]	19.0 ± 0.6[e]							

[a] Ref 19. [b] Ref 3. [c] Ref 4. [d] Ref 5. [e] Ref 6. [f] Ref 7. [g] Ref 13. [h] Ref 8. [i] Ref 9. [j] Ref 10. [k] Ref 11. [l] Ref 12. [m] Ref 18. [n] Ref 16.

TABLE 2: L^{-1} Matrix Elements for the Group IV Hydrides[a] and SiF_4

	CD_4		SiD_4		SiF_4	
	S_3	S_4	S_3	S_4	S_3	S_4
Q_3	1.2851	−0.0062	1.3577	−0.0169	2.8704	0.2792
Q_4	−0.3048	0.8585	−0.1449	1.3703	−2.4770	2.1903

[a] The $\mathbf{L^{-1}}$ elements for CH_4 are taken from ref 19; for SiH_4 from ref 13; for GeH_4 and GeD_4 from ref 9; and for SnH_4 and SnD_4 from ref 11.

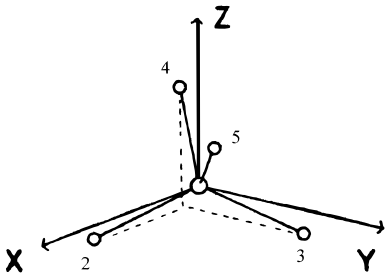

Figure 1. Cartesian coordinate system, molecular orientation, and atom numbering scheme of the MH_4 and SiF_4 molecules.

from refs 3−13, 16, and 18, as well as from the methane study by Mills.[19] These frequency and intensity values are presented in Table 1. The corresponding $\mathbf{L^{-1}}$ matrix elements are given in Table 2. The internal and symmetry coordinate definitions are the same as those in ref 3. The Cartesian coordinate system and molecular orientation and atom numbering scheme are shown in Figure 1.

The polar tensors of the group IV hydrides are represented by a juxtaposition of all the atomic polar tensors (APT)

$$\mathbf{P}_X = [\mathbf{P}_X^{(M)} : \mathbf{P}_X^{(H2)} : ... : \mathbf{P}_X^{(H5)}]$$

where M represents the group IV atoms. For SiF_4, M = Si and F replaces the H symbol. Each atomic polar tensor[20] $\mathbf{P}_X^{(\alpha)}$ is defined by

$$\mathbf{P}_X^{(\alpha)} = \begin{bmatrix} \partial\vec{p}_x/\partial x_\alpha & \partial\vec{p}_x/\partial\vec{y}_\alpha & \partial\vec{p}_x/\partial\vec{z}_\alpha \\ \partial\vec{p}_y/\partial\vec{x}_\alpha & \partial\vec{p}_y/\partial\vec{y}_\alpha & \partial\vec{p}_y/\partial\vec{z}_\alpha \\ \partial\vec{p}_z/\partial\vec{x}_\alpha & \partial\vec{p}_z/\partial\vec{y}_\alpha & \partial\vec{p}_z/\partial\vec{z}_\alpha \end{bmatrix} = \begin{bmatrix} p_{xx}^{(\alpha)} & p_{xy}^{(\alpha)} & p_{xz}^{(\alpha)} \\ p_{yx}^{(\alpha)} & p_{yy}^{(\alpha)} & p_{yz}^{(\alpha)} \\ p_{zx}^{(\alpha)} & p_{zy}^{(\alpha)} & p_{zz}^{(\alpha)} \end{bmatrix}$$

The polar tensors were calculated from experimental intensity data for all possible sign alternatives using the TPOLAR program.[21] Ab initio calculations were carried out using the Gaussian 94[22] and the GAMESS[23] programs on an IBM RISC/6000 workstation network at the São Paulo State High Performance Computer Center (CENAPAD/SP). All the APT ab initio results were obtained using theoretically optimized geometries.

To determine the theoretical dipole moment derivatives for the group IV hydrides, the Stevens, Basch, and Krauss (SBK)[24] and the Hay and Wadt (HW)[25] effective core potentials for the ab initio molecular orbital calculations replaced the innermost electrons of Si, Ge, and Sn. The valence shell basis sets used with the SBK and HW pseudopotentials were changed to a basis set adapted from a universal Gaussian basis set available in the literature.[26] The calculation of dipole moments using either SBK or HW pseudopotentials is not rigorously meaningful since the pseudo-orbitals do not present the correct nodal structure and should be orthogonalized to the core. However, the comparison between all-electron and pseudopotential results indicates that the effect of orthogonalization does not significantly change this property. The resulting valence shell basis sets were composed of (8s8p4d) primitive Gaussian functions determined by the generator coordinate method.[27] The primitives were contracted by the segmented method, giving a [4s4p4d] contracted basis set as shown in Table 3. The carbon and fluorine atoms were given a [4s4p] contracted basis, and an uncontracted (5s4p1d) primitive set was assigned to the hydrogen atoms.

The universal basis set calculations were compared with experimental results and the results obtained from the more familiar MP2/6-311++G(3d,3p) molecular orbital calculations for CH_4, SiH_4, and SiF_4 molecules. For GeH_4 and SnH_4 only experimental results were available to compare with the universal basis set results. Table 4 lists the calculated and experimental equilibrium bond lengths of the group IV hydrides and SiF_4. Note that the universal basis set equilibrium SiH bond length is in excellent agreement with the experimental and MP2/6-311++G(3d,3p) bond lengths. Also the universal basis set results for GeH_4 and SnH_4 are also in excellent agreement with the experimental results. Later we will show that these basis sets also provide excellent estimates of the polar tensor elements for the molecules studied here.

The principal component (PC) method, which has been shown to be useful in the analysis of polar tensor results for resolving derivative sign ambiguities,[28] is also employed here. Since several sets of polar tensor elements, each corresponding to different sets of measured intensities, must be examined for all their $\partial\vec{p}/\partial Q_j$ sign combinations (Q_j is the jth normal coordinate)

TABLE 3: Universal Basis Set Coefficients for the Si, Ge, and Sn Valence Shells as Well as for the Hydrogen and Fluorine Atoms

Si and Ge Basis Set

s		p		d	
exponent	coefficient	exponent	coefficient	exponent	coefficient
0.021 493 6	0.006 624	0.021 493 6	0.007 587	0.090 718 0	1.0
0.044 157 2	0.032 127	0.044 157 2	0.111 506		
				0.186 374 0	1.0
0.090 718 0	0.404 695	0.090 718 0	0.353 277		
0.186 374 0	0.476 784	0.186 374 0	0.388 723	0.382 892 9	1.0
0.382 892 9	0.342 049				
		0.382 892 9	0.257 604	0.786 627 9	1.0
0.786 627 9	−0.210 729	0.786 627 9	0.030 350		
1.616 074 4	−0.162 497	1.616 074 4	−0.046 158		
3.320 116 9	1.0	3.320 116 9	1.0		

Sn Basis Set

s		p		d	
exponent	coefficient	exponent	coefficient	exponent	coefficient
0.021 493 6	−0.012 636	0.0214 936	0.022 638	0.090 718 0	1.0
		0.044 157 2	0.196 705		
0.044 157 2	−0.053 457			0.186 374 0	1.0
0.090 718 0	−0.540 746	0.090 718 0	0.447 227		
0.186 374 0	−0.446 641	0.186 374 0	0.359 896	0.382 892 9	1.0
0.382 892 9	−0.314 318				
		0.382 892 9	1.0	0.786 627 9	1.0
0.786 627 9	0.550 362				
1.616 074 4	−0.044 264	0.786 627 9	−0.133 896		
		1.616 074 4	0.001 667		
3.320 116 9	1.0	3.320 116 9	−0.004 134		

H Basis Set

s	sp	d
0.040 63	22.963 2	3.463 75
	3.463 75	
	0.784 75	
	0.197 72	

F Basis Set

s		p	
exponent	coefficient	exponent	coefficient
13 000.719 746 16	0.002 233 2	106.016 336 48	0.012 241 7
4500.530 240 32	0.004 097 0	36.872 322 43	0.049 281 6
1557.973 161 45	0.019 835 9	12.824 138 30	0.236 781 7
539.332 088 04	0.069 791 6	4.460 216 02	0.792 245 5
186.703 537 90	0.241 242 9		
64.632 184 58	0.741 670 7	1.551 256 43	0.460 940 7
		0.539 524 65	0.473 261 1
22.374 076 73	1.0	0.187 645 86	0.214 168 0
7.745 356 48	1.0		
2.681 252 40	0.137 063 1		
0.928 183 81	0.570 108 7		
0.321 314 46	0.368 596 8		

and compared to ab initio results as well as to polar tensor elements corresponding to the sign alternatives of their deuterated hydrides, the application of this dimensionality reduction technique is especially convenient. Besides permitting a visual comparison of the experimental and theoretical values, the PC graphs clearly display the variations in the polar tensor elements due to different experimental intensity results as well as to variations owing to the various $\partial\vec{p}/\partial Q_j$ sign alternatives. The former variations are expected to be much smaller than the latter ones, facilitating sign determination for most applications.

Polar tensor element errors are propagated to the principal component values and are indicated by the size of the symbols in the principal component graphs. Overlapping pairs of points for isotopomers correspond to polar tensor values satisfying the isotopic invariance criterion. Correct solutions for the dipole moment derivatives are expected to obey this criterion within the limits of experimental error and also be in good agreement with ab initio estimates.

Results

The triply degenerate infrared-active species of MX_4 molecules has three polar tensor elements that are unique and nonzero. As such, the polar tensor space is tridimensional. Using principal component analysis, this space can be reduced to two dimensions permitting the construction of accurate bidimensional graphs for sign determination. Table 5 contains polar tensor element values obtained from experimental intensities and from ab initio calculations. This table and the principal component graphs are used to obtain preferred polar tensor values.

TABLE 4: Molecular Orbital Results for the Equilibrium Bond Lengths of the MH_4 (M = C, Si, Ge, Sn) and SiF_4 Molecules

			r_{M-H} in MH_4				
basis set			M = C	M = Si	M = Ge	M = Sn	r_{Si-F} in SiF_4
6-311++G(3d,3p)	HF[a]		1.0815	1.4747			1.5475
	MP2		1.0858	1.4731			1.5764
	DFT/B3LYP		1.0884				
[4s4p4d]/(5s4p1d)	HF	HW[b]		1.460	1.533	1.702	
		SBK		1.474	1.520	1.693	
	MP2	HW		1.456	1.530	1.698	
		SBK		1.470	1.518	1.689	
[4s4p4d]/[4s2p]	HF	HW					1.545
		SBK					1.556
	MP2	HW					1.552
		SBK					1.563
expt[32]			1.09	1.48	1.527	1.701	1.561

[a] Calculational level. [b] Effective core potentials.

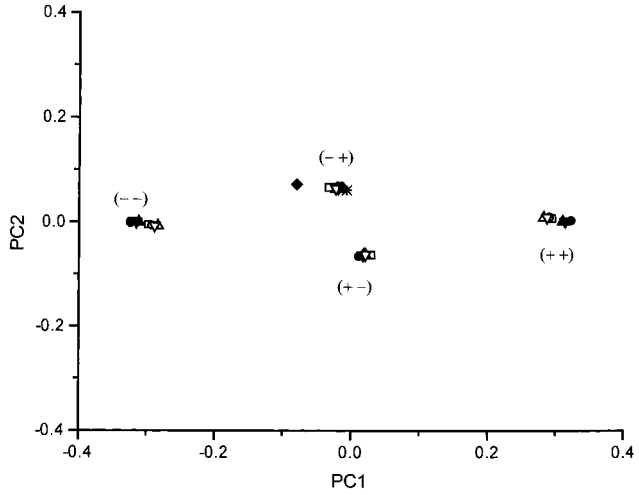

Figure 2. Principal component score graph of the methane polar tensor elements as a function of the signs of the $\partial\vec{p}/\partial Q_j$. CH_4 (■) and CD_4 (□) intensities from ref 3; CH_4 (●) and CD_4 (○) intensities from ref 4; CH_4 (▲) and CD_4 (△) intensities from ref 5; CH_4 (▼) and CD_4 (▽) intensities from ref 6; (◆) HF/6-311G++(3d,3p); (*) MP2/6-311++G(3d,3p); (+) B3LYP/6-311++G(3d,3p). This graph contains 100% of the total data variance.

Methane. The principal component graph of the atomic polar tensor elements of the CH_4 and CD_4 molecules is shown in Figure 2. The four groups of experimental points correspond to the four possible alternative sign combinations for the $\partial\vec{p}/\partial Q_3$ and $\partial\vec{p}/\partial Q_4$ derivatives. The (− +) and (+ −) alternative groups contain H−D pairs satisfying the isotopic invariance criterion, as shown by the overlapping points for the isotopomers. Of these only the (− +) alternative group has principal component score points for the experimental and theoretical APT results that are all very close to one another and well separated from the points for the other sign alternatives. The values of the corresponding preferred sets of APT elements are presented in Table 5 along with the theoretical values. Averages of these preferred sets of APT elements are the best estimates of the CH_4 tensor values, and their errors are taken to be the standard deviations of the experimental values.

Silane. The principal component graph of the APT values for SiH_4 and SiD_4 is given in Figure 3. The APT score points for the SiH_4 intensity data of refs 8 and 13 overlap with the points obtained from the SiD_4 intensities of ref 8 for the (− −) and (+ +) sign combinations. Furthermore principal component score values for the APTs of ref 7 for SiH_4 and SiD_4 are in close proximity to these scores. The ab initio results are clustered close to the (− −) sign combination results shown in Figure 3. The preferred values of the APTs for silane are then taken to be the averages of the APT values of the (− −) sign alternative corresponding to the data of refs 8 and 13. All these experimentally derived APT values as well as the theoretical values used here are presented in Table 5.

Germane. The principal component graph in Figure 4 shows points derived from the experimental intensity values of refs 9, 10, and 13. They result in overlapping score points for all alternative sign combinations. As such, the isotopic invariance criterion can not be used to determine the correct signs of the $\partial\vec{p}/\partial Q_j$'s. On the other hand the ab initio values are much closer to the results for the (− −) sign alternative and permit its selection as the correct set of signs for the $\partial\vec{p}/\partial Q_j$ values. Table 5 contains the four sets of APT element values for this sign alternative for the GeH_4 and GeD_4 data. The standard deviations of these elements are only 0.01e or less, and their average values are the preferred values of the APTs.

Stannane. The stannane intensity values in Table 1 show large differences between results obtained by Levin[11] and McKean[12] some thirty years ago. Independent determinations performed recently by Coats et al.[13] agree well with McKean's intensity values. As a consequence, the individual polar tensor element results obtained from the SnH_4−SnD_4 results of Levin are quite different than those for SnH_4 of refs 12 and 13 for the (− −) and (+ +) sign alternatives, as can be seen in the principal component graph in Figure 5. The molecular orbital results clearly indicate that the (− −) set of signs is to be preferred over the others. The theoretical values have principal component score points falling between those of ref 11 and those of refs 12 and 13. However the theoretical values, calculated using effective core potentials for the heavy tin atom, are not accurate enough to choose between the different experimental sets of values.

The polar tensor element values preferred here and given in Table 5 were taken to be an average of the results from refs 12 and 13 for the (− −) set of signs. The data of ref 11 was not included in the averaging since it seems that its reported intensities are too high. The Si, Ge, and Sn atoms have similar electronegativities, and one can expect the fundamental intensity sum for SnH_4 to be similar to those of SiH_4 and GeH_4. Whereas the SnH_4 intensity sums of refs 12 and 13 are only about 20−40% larger than those for SiH_4 and GeH_4, those of ref 11 are 2.5−3.9 times as large.

Tetrafluorosilane. Sign determination for SiF_4 can only be made by reference to ab initio results since intensity measurements have only been made on one isotopomer. However sign determination is usually simple for polar molecules, and SiF_4 is no exception. Polar tensor element values for the experimental sign alternatives are given in Table 5 along with

TABLE 5: Preferred Polar Tensor Elements and Their Theoretical Estimates for CH_4, SiH_4, GeH_4, SnH_4, and SiF_4

	$p_{xx}^{(C)}/e$	$p_{xx}^{(H5)}/e$	$p_{xy}^{(H5)}/e$
CH_4 $(-+)^a$	0.016 ± 0.008	-0.004 ± 0.002	-0.067 ± 0.002
CD_4 $(-+)^a$	0.025 ± 0.008	-0.006 ± 0.002	-0.067 ± 0.002
CH_4 $(-+)^b$	0.008 ± 0.008	-0.002 ± 0.002	-0.067 ± 0.002
CD_4 $(-+)^b$	0.015 ± 0.007	-0.004 ± 0.002	-0.065 ± 0.002
CH_4 $(-+)^c$	0.014 ± 0.004	-0.003 ± 0.001	-0.065 ± 0.001
CD_4 $(-+)^c$	0.017 ± 0.009	-0.004 ± 0.002	-0.064 ± 0.002
CH_4 $(-+)^d$	0.014 ± 0.002	-0.003 ± 0.001	-0.065 ± 0.000
CD_4 $(-+)^d$	0.017 ± 0.008	-0.004 ± 0.002	-0.065 ± 0.002
average	0.016 ± 0.005	-0.004 ± 0.001	-0.066 ± 0.001
HF/6-311++G(3d,3p)	0.072	−0.018	−0.077
MP2/6-311++G(3d,3p)	0.002	0.000	−0.061
B3LYP/6-311++G(3d,3p)	0.007	−0.002	−0.066
	$p_{xx}^{(Si)}/e$	$p_{xx}^{(H5)}/e$	$p_{xy}^{(H5)}/e$
SiH_4 $(--)^e$	0.849 ± 0.023	-0.212 ± 0.006	-0.023 ± 0.004
SiD_4 $(--)^e$	0.748 ± 0.017	-0.187 ± 0.004	-0.016 ± 0.003
SiH_4 $(--)^f$	0.891 ± 0.005	-0.223 ± 0.001	-0.015 ± 0.001
SiH_4 $(--)^g$	0.917	−0.229	−0.016
SiD_4 $(--)^g$	0.905	−0.226	−0.015
average^m	0.904 ± 0.013	-0.226 ± 0.006	-0.015 ± 0.004
HF-ECP(HW)/[4s4p4d]/(5s4p1d)	1.029	−0.257	−0.021
HF-ECP(SBK)/[4s4p4d]/(5s4p1d)	1.082	−0.271	−0.023
MP2-ECP(HW)/[4s4p4d]/(5s4p1d)	0.937	−0.234	−0.014
MP2-ECP(SBK)/[4s4p4d]/(5s4p1d)	0.991	−0.248	−0.016
MP2/6-311++G(3d,3p)	1.008	−0.252	−0.020
	$p_{xx}^{(Ge)}/e$	$p_{xx}^{(H5)}/e$	$p_{xy}^{(H5)}/e$
GeH_4 $(--)^h$	0.859 ± 0.008	-0.215 ± 0.002	-0.036 ± 0.002
GeD_4 $(--)^h$	0.850 ± 0.003	-0.212 ± 0.001	-0.039 ± 0.001
GeH_4 $(--)^f$	0.871 ± 0.009	-0.218 ± 0.002	-0.039 ± 0.002
GeH_4 $(--)^i$	0.867	−0.217	−0.040
average	0.862 ± 0.009	-0.216 ± 0.003	-0.039 ± 0.002
HF-ECP(HW)/[4s4p4d]/(5s4p1d)	1.124	−0.281	−0.040
HF-ECP(SBK)/[4s4p4d]/(5s4p1d)	1.116	−0.279	−0.046
MP2-ECP(HW)/[4s4p4d]/(5s4p1d)	1.030	−0.257	−0.033
MP2-ECP(SBK)/ [4s4p4d]/(5s4p1d)	1.021	−0.255	−0.039
	$p_{xx}^{(Sn)}/e$	$p_{xx}^{(H5)}/e$	$p_{xy}^{(H5)}$/e
SnH_4 $(--)^j$	1.460 ± 0.011	-0.365 ± 0.003	-0.066 ± 0.002
SnD_4 $(--)^j$	1.471 ± 0.031	-0.368 ± 0.008	-0.060 ± 0.004
SnH_4 $(--)^f$	1.038 ± 0.004	-0.260 ± 0.001	-0.043 ± 0.001
SnH_4 $(--)^k$	0.993	−0.248	−0.051
average^m	1.016 ± 0.032	-0.254 ± 0.008	-0.047 ± 0.006
HF-ECP(HW)/[4s4p4d]/(5s4p1d)	1.373	−0.343	−0.042
HF-ECP(SBK)/[4s4p4d]/(5s4p1d)	1.328	−0.332	−0.044
MP2-ECP(HW)/[4s4p4d]/(5s4p1d)	1.277	−0.319	−0.037
MP2-ECP(SBK)/[4s4p4d]/(5s4p1d)	1.232	−0.308	−0.039
	$p_{xx}^{(Si)}/e$	$p_{xx}^{(F5)}/e$	$p_{xy}^{(F5)}/e$
SiF_4 $(--)^l$	2.215 ± 0.111	-0.554 ± 0.028	-0.070 ± 0.030
HF-ECP(HW)/[4s4p4d]/[4s2p]	2.536	−0.634	−0.062
HF-ECP(SBK)/[4s4p4d]/[4s2p]	2.543	−0.636	−0.061
MP2-ECP(HW)/[4s4p4d]/[4s2p]	2.674	−0.668	−0.128
MP2-ECP(SBK)/[4s4p4d]/[4s2p]	2.281	−0.570	−0.068
MP2/6-311++G(3d,3p)	2.407	−0.602	−0.137

[a] Calculated using intensities of ref 3. [b] Calculated using intensities of ref 4. [c] Calculated using intensities of ref 5. [d] Calculated using intensities of ref 6. [e] Calculated using intensities of ref 7. [f] Ref 13. [g] Calculated using intensities of ref 8. [h] Calculated using intensities of ref 9. [i] Calculated using intensities of ref 10. [j] Calculated using intensities of ref 11. [k] Calculated using intensities of ref 12. [l] Calculated using intensities of ref 16. [m] Average of results from ref 8 and 13. Errors in average values are calculated from their standard deviations except when a propagated error is larger. [n] Average of results from ref 12 and 13.

theoretical results for four different wave functions. All the theoretical results are clearly in best agreement with $(--)$ sign alternative for the SiF_4 derivatives. Its polar tensor element values are taken to be the preferred ones for SiF_4.

Discussion

As stated earlier, the carbon mean dipole moment derivatives, $\bar{p}_C$, of a group of carbon-containing compounds have been related to their carbon 1s electron binding energies,[1] $E_{1s,C}$, using a simple potential model proposed earlier by Siegbahn and collaborators,[2]

$$E_{1s,C} = k_C\bar{p}_C + V \quad \text{with} \quad V = \sum_{B\neq C} \bar{p}_B/R_{BC}$$

In this equation, mean dipole moment derivatives replace the atomic charges used in the original proposition of this model. The second term on the right-hand side represents the electrostatic potential (V) at the nucleus of the carbon atom owing to

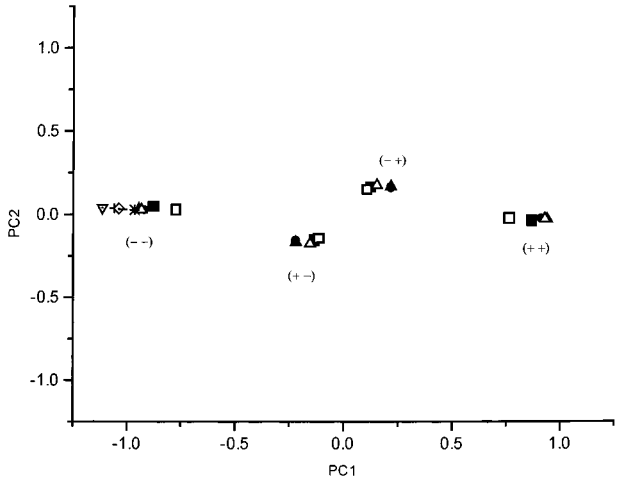

Figure 3. Principal component score graph of the silane polar tensor elements as a function of the signs of the $\partial\vec{p}/\partial Q_j$. SiH_4 (■) and SiD_4 (□) intensities from ref 7; SiH_4 (●) intensities from ref 13; SiH_4 (▲) and SiD_4 (△) intensities from ref 8; (+) HF-ECP(HW)/[4s4p4d]/(5s4p1d); (▽) HF-ECP(SBK)/[4s4p4d]/(5s4p1d); (*) MP2-ECP(HW)/[4s4p4d]/(5s4p1d); (−) MP2-ECP(SBK)/[4s4p4d]/(5s4p1d); (◇) MP2/6-311++G(3d,3p). This graph contains 100% of the total data variance.

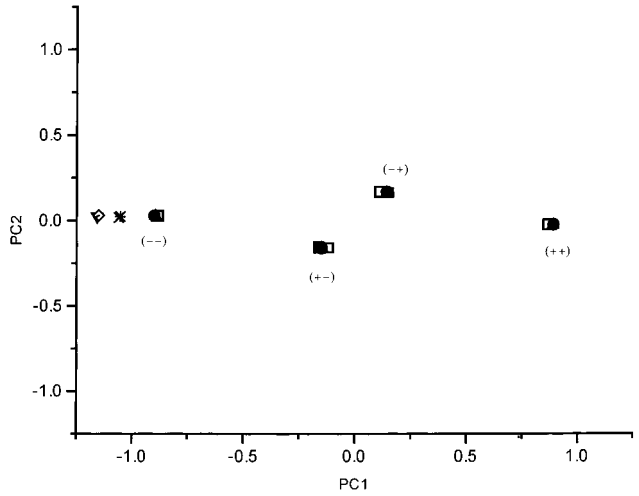

Figure 4. Principal component score graph of the germane polar tensor elements as a function of the signs of the $\partial\vec{p}/\partial Q_j$. GeH_4 (■) and GeD_4 (□) intensities from ref 9; GeH_4 (●) intensities from ref 13; GeH_4 (▲) intensities from ref 10; (▽) HF-ECP(HW)/[4s4p4d]/(5s4p1d); (◇) HF-ECP(SBK)/[4s4p4d]/(5s4p1d); (+) MP2-ECP(HW)/[4s4p4d]/(5s4p1d); (*) MP2-ECP(SBK)/[4s4p4d]/(5s4p1d). This graph contains 100% of the total data variance.

the charges of the neighboring atoms with R_{BC} being the internuclear distance between atoms B and C. The value of k_C can be identified with the Coulomb repulsion integral between a core and a valence electron on the atom involved in the ionization process.

Here, this potential model is investigated using the 2p electron binding energies and mean dipole moment derivatives of the silicon atoms in silane and tetrafluorosilane. The experimental Si 2p binding energies and mean dipole moment derivatives of SiH_4 and SiF_4 are presented in Table 6. The values of these binding energies corrected for the neighboring atom electrostatic potentials and the ones also corrected for the relaxation energies (E_{rel}) are plotted against the Si mean dipole moment derivatives in Figure 6. If the simple potential model is valid for these data, the points for SiH_4 and SiF_4 would be connected by the dotted line shown in this figure. Unfortunately neither electron

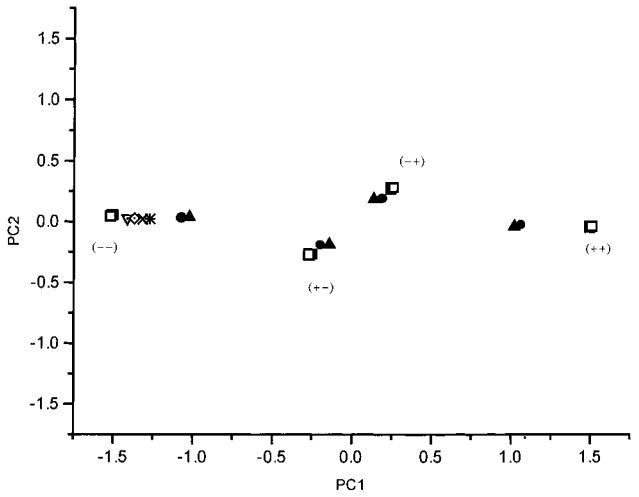

Figure 5. Principal component score graph of the stannane polar tensor elements as a function of the signs of the $\partial\vec{p}/\partial Q_j$. SnH_4 (■) and SnD_4 (□) intensities from ref 11; SnH_4 (●) intensities from ref 13; SnH_4 (▲) intensities from ref 12; (▽) HF-ECP(HW)/[4s4p4d]/(5s4p1d); (◇) HF-ECP(SBK)/[4s4p4d]/(5s4p1d); (+) MP2-ECP(HW)/[4s4p4d]/(5s4p1d); (*) MP2-ECP(SBK)/[4s4p4d]/(5s4p1d). This graph contains 100% of the total data variance.

TABLE 6: Mean Dipole Moment Derivatives of C, Si, Ge, and Sn and 2p Electron Binding Energies for the Fluorosilanes and the Fluorogermanes and Their Relaxation Energies. M is the Central Atom

	experimental			theoretical[a] ΔSCF	
	$\bar{p}_M/e$	$E_{M,2p}$/eV[b]	p_M/e[c]	$E_{M,2p}$/eV	$-E_{rel}$/eV
CH_4	0.016				
SiH_4	0.904	107.28	1.008	106.93	8.09
SiH_3F			1.448	108.24	7.84
SiH_2F_2			1.806	109.55	7.50
$SiHF_3$			2.106	110.69	7.37
SiF_4	2.215	111.79	2.407	111.86	7.21
GeH_4	0.862	129.33	1.027	132.47	7.83
GeH_3F			1.416	133.82	7.61
GeH_2F_2			1.725	134.90	7.57
$GeHF_3$			1.991	136.21	7.29
GeF_4		133.75	2.271	137.43	7.18
SnH_4	1.016				

[a] 6-311++G(3d,3p) basis set was used for the fluorosilanes and A-VDZ/6-311++G(3d,3p) basis set for the fluorogermanes as indicated in the text. [b] Data from ref 31. [c] Values calculated at the MP2 level with the same basis sets as the ones used for the ΔSCF energies.

binding energy nor infrared intensity data are available for any of the other fluorosilanes, SiH_3F, SiH_2F_2 and $SiHF_3$.

To test the validity of the potential model for the silicon atom, MP2/6-311++G(3d,3p) dipole moment derivative calculations were carried out for the fluorosilanes. Si atom 2p ionization and relaxation energies of the fluorosilanes using the same basis set at the Hartree−Fock level were calculated using the ΔSCF method.[29] These energy and dipole moment derivative values are presented in Table 6 along with the available experimental values. Note that the ΔSCF 2p ionization energies are in good agreement with the experimental values. Also excellent agreement between the ab initio and experimentally derived mean dipole moment derivatives has been commented on in the previous section. The corresponding simple potential model graphs for the theoretical values, $E_{2p,Si} - V$ and $E_{2p,Si} - V - E_{rel}$, vs $\bar{p}_{Si}$ are also shown in Figure 6. The theoretical values are situated on straight lines as expected for the potential model, whether the relaxation energy correction is included or not. Furthermore the slope of the line for the theoretical points including the relaxation energy, 11.56 eV/e, is almost the same

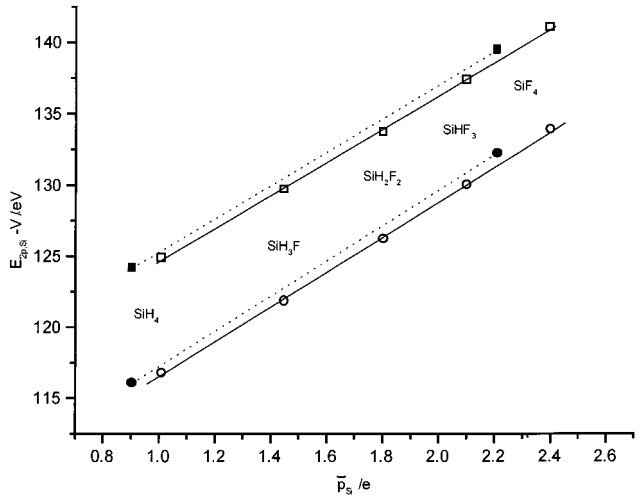

Figure 6. Silicon 2p electron binding energies corrected for the neighboring atom electrostatic potential graphed against the silicon mean dipole moment derivatives: (●) experimental values; (○) MP2/6-311++G(3d,3p); (■) experimental values corrected for the relaxation energies; (□) MP2/6-311++G(3d,3p) values corrected for the relaxation energies.

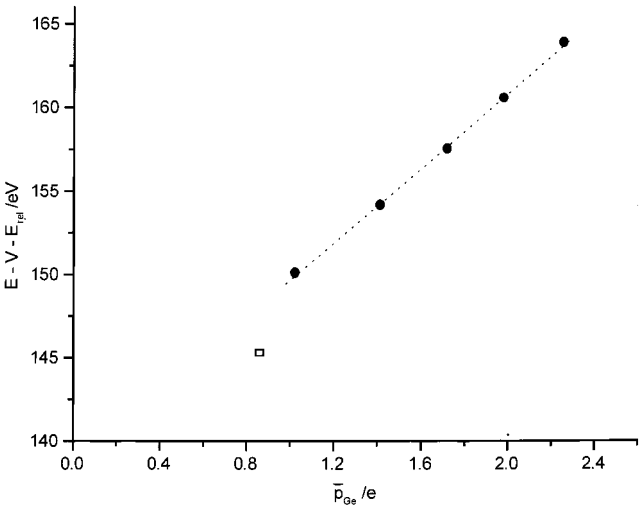

Figure 7. Germanium 3p electron binding energies corrected for the neighboring atom electrostatic potential and the relaxation energies graphed against the germanium mean dipole moment derivatives. (●) MP2/A-VDZ/6-311++G(3d,3p) dipole moment derivatives and ΔSCF energy values; (□) experimental values.

as the slope obtained from the two relaxation energy corrected experimental points of SiH_4 and SiF_4, 11.66 eV/e. Note that the experimental and theoretical lines are displaced by only a few tenths of an electronvolt. Also the slopes for the potential model lines obtained without using the relaxation energy corrections are very similar to the above, as is clearly seen in Figure 6.

This argument can be extended to the germane atom if theoretical energies and mean dipole moment derivatives of the fluorogermanes are used. Their values were calculated in the same way as for the silanes with Hartree−Fock and Möller−Plesset two-level wave functions with an A-VDZ basis for the germane atom and 6-311++G(3d,3p) basis for the terminal atoms. The results have been included in Table 6, and the fluorogermane potential model plot is shown in Figure 7. As seen there, these theoretical values also adhere to the simple potential model. Unfortunately intensity data are only available for GeH_4.

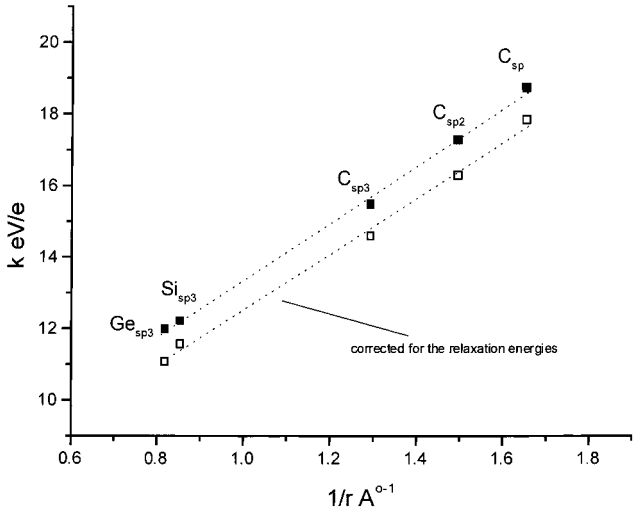

Figure 8. Slopes of the potential model equation against the inverses of the covalent radii.

The proportionality constant for the potential model, *k*, is expected to be a measure of the average electrostatic interaction energy between a core and valence electron. Assuming that the core electron is very close to the nucleus, one expects that the slope of the potential model equation would vary inversely with the covalent radius of the atom. This relationship was found to be obeyed for carbon atoms with different hybridization states in our earlier investigation.[1] In Figure 8 the potential model slopes are graphed against their corresponding covalent radii[30] for the sp, sp^2, and sp^3 hybrid carbon atoms, the sp^3 Si atom, and the sp^3 Ge atom. Indeed all the points do fall on a straight line as expected, confirming the proposition that the Si 2p and Ge 3p core electron binding energies, as well as the 1s carbon energies, obey the simple potential model if the atomic charges are substituted by mean dipole moment derivatives.

For 1.22 Å covalent radius[30] of Ge the relationship in Figure 8 for relaxation energy corrected values predicts a potential model slope of 11.12 eV/e. The slope of the corresponding line in Figure 7 is in excellent agreement, 11.07 eV/e. Even though our calculated ionization energies are a few electronvolts more than the experimental ones, evidently owing to deficiencies in our treatment of the relaxation effects, the line slopes are not affected. As has been often assumed in earlier studies of core binding energies, the relaxation energies are practically constant for similar molecules.

Furthermore, experimental 3d electron ionization energy values[31] for GeH_4, 37.40 eV, and GeF_4, 42.05 eV, suggest the validity of the potential model expressed in terms of mean dipole moment derivatives. Their difference, 4.55 eV, is about a tenth of an electronvolt larger than the difference between the corresponding 3p energy values (see Table 6). Unfortunately, core electron ionization energies have not been reported for SnF_4, so these arguments cannot be extended to the tin atom at this time.

The success of the simple potential model expressed in terms of mean dipole moment derivatives implies that the latter quantity can be interpreted as an atomic charge for the group IV atoms. As can be seen in Table 6, this quantity is almost zero for carbon in methane ($0.016 \pm 0.005e$) and much higher for silicon ($0.904 \pm 0.013e$) and germane ($0.862 \pm 0.009e$) in the group IV hydrides. Note that the silicon atomic charge is predicted be slightly higher than the germane charge. The tin charge, $1.016 \pm 0.32e$, appears to be the highest for the group IV atoms in their hydrides.

TABLE 7: Rotated Preferred Polar Tensor Elements[a]

	$p^{(H5,F5)}_{x'x'}/e$	$p^{(H5,F5)}_{z'z'}/e$
CH_4	0.062	−0.136
SiH_4	−0.211	−0.256
GeH_4	−0.177	−0.294
SnH_4	−0.207	−0.348
SiF_4	−0.484	−0.694

[a] The z'- and x'-axes are parallel and perpendicular to the M−H5 or Si−F5 bond.

An explanation for the inversion of silicon and germane mean dipole moment derivative values can be made using the very simple bond moment model. The preferred terminal atom polar tensors can be rotated such that one axis lies along a bond and the other two axes are perpendicular to it. Transformed H and F preferred polar tensor elements corresponding to a coordinate system with the z'-axis along the M−H or M−F bond and the x'-axis perpendicular to it are presented in Table 7. Note that the $p^{(H5)}_{z'z'}$ tensor element is always negative and its magnitude increases monotonically as the central atom becomes heavier. The simple bond moment hypothesis interprets these values as charge fluxes, the flux increasing as the atomic number of the central atom increases. On the other hand this model interprets the $p^{(H5)}_{x'x'}$ element as equilibrium atomic charge. Its magnitude in SiH_4 is larger than in GeH_4. This would imply that the Si atomic charge in SiH_4 is more positive than the Ge charge in GeH_4, just as many inorganic chemists have suspected. As such, the inversion in Si and Ge mean dipole moment derivative values indeed appears to have its origin in a static equilibrium charge contribution.

Acknowledgment. The authors thank the Fundação de Amparo à Pesquisa do Estado de São Paulo (FAPESP) and the Conselho Nacional de Pesquisa (CNPq) for partial financial support. A.E.O. and P.H.G. thank CNPq for doctoral fellowships. The authors thank one of the referees for very helpful suggestions.

References and Notes

(1) Guadagnini, P. H.; Oliveira, A. E.; Bruns, R. E.; de Barros Neto, B. *J. Am. Chem. Soc.* **1997**, *119*, 4224.

(2) Siegbahn, K.; Nordling, C.; Johansson, G.; Hedman, J.; Hedén, P. F.; Hamrin, K.; Gelius, U.; Bergmark, T.; Werne, L. O.; Manne, R.; Baer, Y. *ESCA Applied To Free Molecules*; North-Holland Publishing Company: Amsterdam, 1971.

(3) Heicklen, J. *Spectrochim. Acta* **1961**, *17*, 201.

(4) Saëki, S.; Mizuno, S.; Kondo, S. *Spectrochim. Acta* **1976**, *32A*, 403.

(5) Bode, J. H. G.; Smit, W. M. A. *J. Phys. Chem.* **1980**, *84*, 198.

(6) Kim, K. *J. Quantum Spectrosc. Radiat. Transfer* **1987**, *37*, 107.

(7) Levin, I. W.; King, W. T. *J. Chem. Phys.* **1962**, *37*, 1375.

(8) Ball, D. F.; McKean, D. C. *Spectrochim. Acta* **1962**, *18*, 1029.

(9) Levin, I. W. *J. Chem. Phys.* **1965**, *42*, 1244.

(10) Chalmers, A. A.; McKean, D. C. *Spectrochim. Acta* **1965**, *21*, 1941.

(11) Levin, I. W. *J. Chem. Phys.* **1967**, *46*, 1176.

(12) McKean, D. C. *Chem. Commun.* **1966**, 146.

(13) Coats, A. M.; McKean, D. C.; Steele, D. *J. Mol. Struct.* **1994**, *320*, 269.

(14) Mardia, K. V.; Kent, J. T.; Bibby, J. M. *Multivariate Analysis*; Academic Press: London, 1979; Chapter 8.

(15) Elschenbroich, C. L.; Salzer, A. *Organometallics: A Concise Introduction*; VCH Publishers: Weinheim, Germany, 1992; p 94.

(16) Schartz, P. N.; Hornig, D. F. *J. Chem. Phys.* **1953**, *21*, 1516.

(17) Guadagnini, P. H.; Bruns, R. E. *J. Am. Chem. Soc.* **1995**, *117*, 4144.

(18) McDowell, R. S.; Reisfield, M. J.; Patterson, C. W.; Krohn, B. J.; Vasquez, M. C.; Laguna, G. A. *J. Chem. Phys.* **1982**, *77*, 4337.

(19) Mills, J. M. *Mol. Phys.* **1958**, *1*, 107.

(20) Person, W. B.; Newton, J. H. *J. Chem. Phys.* **1974**, *61*, 1040.

(21) Bassi, A. B. M. S. Doctoral Thesis, Universidade Estadual de Campinas, 1975.

(22) Frisch, M. J.; Trucks, G. W.; Schlegel, H. B.; Gill, P. M. W.; Johnson, B. G.; Robb, M. A.; Cheeseman, J. R.; Keith, T.; Petersson, G. A.; Montgomery, J. A.; Raghavachari, K.; Al-Laham, M. A.; Zakrzewski, V. G.; Ortiz, J. V.; Foresman, J. B.; Cioslowski, J.; Stefanov, B. B.; Nanayakkara, A.; Challacombe, M.; Peng, C. Y.; Ayala, P. Y.; Chen, W.; Wong, M. W.; Andres, J. L.; Replogle, E. S.; Gomperts, R.; Martin, R. L.; Fox, D. J.; Binkley, J. S.; Defrees, D. J.; Baker, J.; Stewart, J. P.; Head-Gordon, M.; Gonzalez, C.; Pople, J. A.; *Gaussian 94*, Revision D.2; Gaussian, Inc.: Pittsburgh PA, 1995.

(23) Schmidt, M. W.; Baldridge, K. K.; Boatz, J.A.; Elbert, S. T.; Gordon, M. S.; Jensen, J. H.; Koseki, S.; Matsunaga, N.; Nguyen, K. A.; Su, S. J.; Windus, T. L.; Dupuis, M.; Montgomery, J. A. *J. Comput. Chem.* **1993**, *14*, 1347.

(24) Stevens, W. J.; Basch, H.; Krauss, M. *J.Chem. Phys.* **1984**, *81*, 6026.

(25) Hay, P. J.; Wadt, W. R. *J. Chem.Phys.* **1985**, *82*, 270.

(26) Malli, G. L.; da Silva, A. B. F.; Ishikawa, Y. *Phys. Rev.* **1993**, *47*, 143.

(27) Giordan Santos, M.; Custódio, R.; Morgon, N. H. *Chem. Phys. Lett.* **1997**, *279*, 396.

(28) Suto, E.; Ferreira, M. M. C.; Bruns, R. E. *J. Comp. Chem.* **1991**, *12*, 885; Suto, E.; Bruns, R. E.; Neto, B. B. *J. Phys. Chem.* **1991**, *95*, 9716.

(29) Bagus, P.S. *Phys. Rev.* **1965**, *A619*, 139.

(30) Pauling, L. *The Nature of the Chemical Bond*, 3rd ed.; Cornell University Press: 1960; p 224.

(31) Jolly, W. L.; Bomben, K. D.; Eyermann, C. J. *Atomic Data and Nuclear Data Tables* **1984**, *31*, 433.

(32) Sutton, L. E., Phil, D., Eds. *Tables of Interatomic Distances and Configurations in Molecules and Ions*, Special Publication, no. 18; The Chemical Society Burlington House: London, 1965.